International Journal of Industrial Engineering Computations 9 (2018) 535–550

Contents lists available at GrowingScience

International Journal of Industrial Engineering Computations

homepage: www.GrowingScience.com/ijiec

Integrated planning of electric vehicles routing and charging stations location considering transportation networks and power distribution systems

Andrés Arias[a], Juan D. Sanchez[a] and Mauricio Granada[a*]

[a]*Program of Electrical Engineering, Technological University of Pereira, Pereira, Colombia*

C H R O N I C L E

Article history:
Received June 18 2017
Received in Revised Format August 25 2017
Accepted November 7 2017
Available online November 7 2017

Keywords:
Electric Vehicle
Capacitated Vehicle Routing Problem
Transportation network, power distribution system
Electric Vehicle Charging Station

A B S T R A C T

Electric Vehicles (EVs) represent a significant option that contributes to improve the mobility and reduce the pollution, leaving a future expectation in the merchandise transportation sector, which has been demonstrated with pilot projects of companies operating EVs for products delivering. In this work a new approach of EVs for merchandise transportation considering the location of Electric Vehicle Charging Stations (EVCSs) and the impact on the Power Distribution System (PDS) is addressed. This integrated planning is formulated through a mixed integer non-linear mathematical model. Test systems of different sizes are designed to evaluate the model performance, considering the transportation network and PDS. The results show a trade-off between EVs routing, PDS energy losses and EVCSs location.

1. Introduction

In the last years, the reduction of the negative impact on the environment produced by the transportation sector has been identified as a relevant issue. According to surveys of Environmental Protection Agency, release of Green House Gases (GHG) provided by the non-renewable energy sources and its derivatives, contribute to 14% of the global pollution (Intergovernmental Panel on Climate Change. Working Group III and Edenhofer n.d.). As established in the road map of Energy Technologies Perspectives, carbon dioxide emissions will be reduced up to 50% by 2050, compared to levels presented in 2005. The 30% of this reduction depends directly by the transportation sector, due to a high penetration of Electric Vehicles (EVs) forecasted by 2050 worldwide and the friendly alternative that this transportation mean can provide to the environment, in comparison with vehicles propelled by internal combustion engines (Tanaka, 2011). Due to the low efficiency of internal combustion engines and increase of cities urbanization rate, EV has become into a more attractive transportation mean, granting possible solutions to worldwide problems that involve the environment, electric power supply and mobility. Some of the advantages provided by EVs are listed below:

- Represent a clean transportation in urban areas.

* Corresponding author
E-mail: magra@utp.edu.co (M. Granada)

2018 Growing Science Ltd.
doi: 10.5267/j.ijiec.2017.10.002

- Permit to obtain a balance close to zero in carbon dioxide emissions release, from the electric power generation source to the EV tire, as long as the electricity has been generated with renewable sources.
- Provide a significant noise reduction.
- Contribute to the expansion of Smart Grid concept, considering decentralized energy storage and demand response.
- Accelerate the development of policies that stimulates the hourly tariff implementation, as a result of the reinjection of the energy stored in the EVs to the Power Distribution System (PDS), applying V2G (Vehicle to Grid) concept.

Since the point of view of the cost-benefit relationship, EVs are not as competitive as conventional vehicles are; respect to drive range, costs and availability of refueling stations. This overview may change at short term due to penalization policies imposed for overcoming the limit of GHG. In this regards, from 2019, European Union will impose a 95 Euros fine to vehicles with emissions greater than 147 grams of CO2 per kilometer traveled (Mock, 2014). During the last decades, the EVs population has been increased rapidly, and its development has reached great maturity (Chan, 1999). Some studies estimate that by 2030 the proportion of EVs will be around 64% of the total of light vehicles (Du et al., 2010). In the transportation sector, the companies are highly responsible to reduce the GHG emissions, emerging several pilot projects for load transportation with EVs in multinational companies such as DHL, FedEx and UPS, where EVs have been included for routing planning.

Despite the above, the emerging of EVs as the main transportation mean is still overshadowed by the low driving range (in comparison with internal combustion engines vehicles), provided by the lithium-ion batteries that lead the EVs energy storage market. The improvement for this type of batteries, in terms of driving range increase, is greatly hampered by issues related with safety, cost, operation temperature and availability of materials (Hannan et al., 2017), which implies that the EVs driving range will not widely improve for the coming years.

Under these circumstances, charging stations play an important role on the electric mobility, allowing to travel longer distances by indirectly increasing EV driving range. In this manner, it is necessary to perform an appropriate siting of Electric Vehicle Charging Stations (EVCSs), as this type of installations are strategic for the massive incorporation of EVs, reaching driving ranges comparable with conventional vehicles. Furthermore, optimal siting of EVCSs does not depend exclusively on the transportation network requirements, because those installations imply large consumptions of electricity. Therefore, the effect of the charging stations on the power distribution networks has to be taken into account, in order to avoid congestion or additional costs associated with energy losses.

A review of the state of the art related with the interaction between electric vehicles and power grids considering EVCSs is done in (Andres et al., 2016). The authors conclude that in the specialized literature, the problem of siting and sizing of EVs charging stations has been slightly addressed. Among the more highlighted works, (Worley et al., 2012) and (Neyestani et al., 2015) are prominent. In (Worley et al., 2012) a EVCSs planning is implemented based on routing models without considering the power distribution system. In (Liu et al., 2012), an EVCSs location strategy was developed considering the costs associated with infrastructure investment and energy losses in the power network. By the other side, in (Pazouki et al., 2015) and (Neyestani et al., 2015) the optimal location of EVCSs is performed taking into account distributed generation (DG). In (Pazouki et al., 2015), the joint location of EVCSs and DG does not only reduces the carbon emissions, but also decreases the power losses of the power system and investment costs of infrastructure. The authors in (Neyestani et al., 2015) conclude that the benefits provided by EVCSs, are node-sensitive in which they are installed, and their location has to be treated holistically with the power system.

Other important publications can be found, such as (Shojaabadi et al., 2016) where the optimal planning of EVCSs is done considering customer's participation in demand response programs and uncertainties associated with load values, arrival time of EVs to EVCSs, initial state of charge of EVs' batteries and electricity market price. Based on a shared nearest neighbor clustering algorithm and queuing theory, the authors in (Dong et al., 2016) have developed a planning method, which is decomposed into three parts: a spatial-temporal model of EVs charging points, a location determination model and a capacity determination model. Distribution network is not taken into account in the planning method, due to the long distance between any two EVCSs and each of them is supplied by a separate distribution network. In contrast with (Dong et al., 2016), in (Luo et al., 2015) the PDS and transportation network graphs are considered, in conjunction with EV owners, urban infrastructure and EVCSs. This way, a multi-stage charging station placement strategy with incremental EV penetration rates is formulated, applying a Bayesian game framework to analyze the strategic interactions among EVCSs service providers.

In this work, the Electric Vehicles Integrated Planning Problem (EVs-IPP) for cargo transportation is presented. The optimal location of EVCSs is performed considering the mobility of cargo EVs along the transportation network and the impact on the PDS. This results as a consequence of the poor capacity that may be presented on the EVs' battery to provide enough autonomy to complete the routes adequately, since the EVs are part of merchandise transport where considerable distances are traveled too often. By the other side, EVCSs represent huge additional loads for the electric network, being the proper location of this type of loads a critical aspect when the energy losses of the PDS are assessed.

A mixed integer non-linear mathematical model is proposed to portray the EVs mobility with the well-known Capacited Vehicle Routing Problem (CVRP) and the distribution system operation with the power flow equations. In this manner, costs associated with cargo EVs routing, EVCSs installation and energy losses are minimized, obtaining an optimal operation in the transportation and electric networks. Additionally, the introduction of a consistent penalty in the objective function helps to determine until what level the current EVs' battery autonomy is suitable to perform the routes. Regardless the battery autonomy, the mathematical model tends to be feasible, as long as this term is not greatly weighted in the objective function. This way, under a non-sufficient battery autonomy scenario, the decision maker can realize that EVCSs installation is not enough to meet the needs of EVs routing, being necessary to replace current batteries for others with larger drive range.

This paper is organized as follows: Section 2 shows the proposed mathematical model of EVs-IPP. Later, section 3 details the test systems used to evaluate the EVs-IPP performance, coupling instances of transportation networks and PDS from the specialized literature. In section 4, the results for different scenarios are depicted. Finally the conclusions of the work are presented in section 5.

2. EVs-IPP formulation

The integrated planning problem proposed in this work, can be formulated as a graph theory problem. Let $G=(V,A)$ a complete graph, where $V=C\cup N$ is the vertices set of the integrated problem and A is the arc set that interconnects all the vertices. Set $C=\{1,\ldots,c\}$ represents the customers vertices and conform the cargo transportation network. Set $N=\{c+1,\ldots,c+n\}$ represents the power demand vertices and conform the PDS. Set $J\subseteq N$ contains all the candidate vertices to install EVCS that in this case is the set of all the nodes except the PDS substations. Sets N and C and their respective arcs can be seen as two disjunctive graphs, and the interaction between these graphs is given by the EVs charging. The EVs are required to meet the customers merchandise demand. PDS vertices of set N are connected each other through lines, which represent the electrical wires, conforming set $L=\{1,\ldots,l\}$.

In this regards, EVs-IPP considers the interaction of three different subproblems. The first subproblem is known in the literature as the Capacitated Vehicle Routing Problem (CVRP), where vehicles fleet with limited cargo capacity leave from a unique depot and deliver merchandise to several customers. The vehicles have to fully meet the merchandise demands, seeking a travelling minimal cost (Christofides, Mingozzi, and Toth 1977). The second subproblem is related with the location of EVCSs, which indirectly provides an increase of the EVs battery range in order to complete the travel satisfactorily. The third subproblem frames the power flow formulation, involving the operation point of the PDS under the additional loads represented by the EVCSs installed.

2.1 Nomenclature

For clarification, the notations used in this paper are listed as follows.

Sets:

C	Set of customers
J	Set of candidate nodes to install EVCSs
$\{0\}$	Depot
$\{0'\}$	Copy of Depot
V	$\{C\} \cup \{J\} \cup \{0\} \cup \{0'\}$
K	Set of electric vehicles
N	Set of nodes belonging the PDS
L	Set of lines belonging the PDS

Parameters:

W_1	Weight factor for EVCSs installation cost term
W_2	Weight factor for routing cost
W_3	Weight factor for penalization term
W_4	Weight factor for energy losses cost
f_h	EVCS installation cost [USD]
fm_h	EVCS maintenance cost [USD]
CPI	Consumer Price Index
nt	Number of years to shift to future value
a_k	Cost per kilometer traveled of vehicle *k* [USD/km]
d_{gh}	Distance between node *g* to node *h* [km]
am_k	Maintenance cost of vehicle *k* to travel one kilometer [USD/km]
ap_k	Cost of the additional capacity of the EV's battery [USD/km]
b	Cost of 1 kWh of energy losses [USD/kWh]
$Loss_{w/oEVCSs}$	Power losses of the PDS without EVCSs installed [kW]
M	Big number
$\lvert K \rvert$	Cardinality of set *K*
q_g	Merchandise demand at customer node *g*
U_k	Merchandise cargo capacity of vehicle *k*
Q	Battery autonomy [km]
P_n^d	Active power demanded at node *n* [kW]
R_{mn}	Resistance of line *mn* belonging the PDS [Ω]
X_{mn}	Reactance of line *mn* belonging the PDS [Ω]
Z_{mn}	Impedance of line *mn* belonging the PDS [Ω]
$V_{\min}$	Lower level of voltage at PDS nodes [V]

$V_{\max}$	Upper level of voltage at PDS nodes [V]
$I_{\max}$	Upper level of current at PDS lines [A]
$P_{\max}^{G}$	Upper level of active power generated at PDS nodes [W]
$PEVCS$	Nominal Active power drawn by EVCS installed [kW]

Variables:

α	Cost of EVCSs installed [USD]
β	Cost of EVs routing at transportation network [USD]
γ	Cost of penalization [USD]
ω	Cost of energy losses at PDS [USD]
y_h	Binary decision variable for EVCS installation at candidate node h. If $y_h=1$ the EVCS is installed and $y_h=0$ otherwise
x_{ghk}	Binary decision variable, taking a value of *1* if vehicle k goes from node g to node h and *0* otherwise
$P_{hk}^{ficticious}$	Missing autonomy to reach node h with vehicle k [km]
i_{mn}^{sqrt}	Square current flowing through line mn of PDS [A^2]
u_{ghk}	Remaining merchandise when vehicle k leaves node g and goes to node h
pb_{hk}^{1}	Battery autonomy before vehicle k arrives node h [km]
pb_{gk}^{2}	Battery autonomy after vehicle k leaves node g [km]
P_{mn}	Active power flowing line mn of PDS [kW]
P_{n}^{G}	Active power generated at node n [kW]
PE_{n}	Active power drawn by an EVCS installed at node n [kW]
Q_{mn}	Reactive power flowing line mn of PDS [kVar]
Q_{n}^{G}	Reactive power generated at node n [kVar]
V_{m}^{sqr}	Square voltage at node m [V^2]

2.2 EVs-IPP Mathematical Model

The mathematical model for EVs-IPP is presented in equations (1) to (29), considering {0} as the depot where the vehicles start the respective routes and {0'} is a depot copy where the vehicles will complete the routes.

$$\min z = W_1 \cdot \alpha + W_2 \cdot \beta + W_3 \cdot \gamma + W_4 \cdot \omega \tag{1}$$

Subject to:

$$\alpha = \sum_{h \in J} \left(f_h + fm_h \right) \cdot y_h \cdot \left(1 + CPI\right)^{nt} \tag{2}$$

$$\beta = 365 \cdot \sum_{g \in V} \sum_{h \in V} \sum_{k \in K} a_k \cdot d_{gh} \cdot x_{ghk} \cdot \left(1 + am_k\right) \cdot \left(1 + CPI\right)^{nt} \tag{3}$$

$$\gamma = 365 \cdot \sum_{h \in V} \sum_{k \in K} ap_k \cdot P_{hk}^{ficticious} \cdot \left(1 + CPI\right)^{nt} \tag{4}$$

$$\omega = 8760 \cdot b \sum_{mn \in L} \left(i_{mn}^{sqrt} \cdot R_{mn} - Loss_{\text{w/o EVCSs}} \right) \cdot \left(1 + CPI\right)^{nt} \tag{5}$$

$$\sum_{g \in V \setminus \{o'\}, g \neq h} \sum_{k \in K} x_{ghk} = 1 \qquad \forall h \in C \tag{6}$$

$$\sum_{g\in V\setminus\{o'\}}\sum_{g\neq h}\sum_{k\in K} x_{ghk} \le M\cdot y_h \qquad \forall h\in J \qquad (7)$$

$$\sum_{h\in V\setminus\{o\},h\neq g} x_{ghk} - \sum_{h\in V\setminus\{o'\},h\neq g} x_{ghk} = 0 \qquad \forall g\in V\setminus\{o,o'\},\forall k\in K \qquad (8)$$

$$\sum_{h\in V\setminus\{o\}} x_{ohk} - \sum_{h\in V\setminus\{o'\}} x_{ho'k} = 0 \qquad \forall k\in K \qquad (9)$$

$$\sum_{h\in V\setminus\{o\}} x_{ohk} \le 1 \qquad \forall k\in K \qquad (10)$$

$$\sum_{k\in K}\sum_{h\in V\setminus\{o\}} x_{ohk} \le |K| \qquad (11)$$

$$\sum_{g\in V\setminus\{o',j\}} u_{ghk} = \sum_{g\in V\setminus\{o,j\}} u_{hgk} \qquad \forall h\in J,\forall k\in K \qquad (12)$$

$$\sum_{h\in V\setminus\{o,g\}} u_{ghk} \le \sum_{h\in V\setminus\{o',g\}} \left(u_{hgk} - q_g\cdot x_{hgk}\right) + U_k\cdot\left(1-\sum_{h\in V\setminus\{o',g\}} x_{hgk}\right) \qquad \forall g\in C,\forall k\in K \qquad (13)$$

$$0\le u_{ghk}\le U_k\cdot x_{ghk} \qquad \forall g\in V\setminus\{o'\},h\in V\setminus\{o\},g\neq h,k\in K \qquad (14)$$

$$pb^1_{hk}\le pb^2_{gk} - d_{gh}\cdot x_{ghk} + Q(1-x_{ghk}) \qquad \forall g\in V\setminus\{o'\},h\in V\setminus\{o'\},g\neq h,k\in K \qquad (15)$$

$$pb^2_{ok} = Q \qquad \forall k\in K \qquad (16)$$

$$pb^2_{gk} = Q\cdot y_g \qquad \forall g\in J \qquad (17)$$

$$pb^2_{hk} = pb^1_{hk} + P^{ficticious}_{hk} \qquad \forall h\in C \qquad (18)$$

$$pb^1_{hk}\ge 0 \qquad \forall h\in V \qquad (19)$$

$$y_j, x_{ghk}\in\{0,1\} \qquad \forall j\in J,\forall g\in V\setminus\{o'\},\forall h\in V\setminus\{o\},\forall k\in K \qquad (20)$$

$$\sum_{mn\in L} P_{mn} - \sum_{nr\in L}(P_{nr} + i^{sqrt}_{nr}\cdot R_{nr}) + P^G_n = P^d_n + PE_n \qquad \forall m\in N,\forall n\in N,\forall r\in N \qquad (21)$$

$$\sum_{mn\in L} Q_{mn} - \sum_{nr\in L}(Q_{nr} + i^{sqrt}_{nr}\cdot X_{nr}) + Q^G_n = Q^d_n \qquad \forall m\in N,\forall n\in N,\forall r\in N \qquad (22)$$

$$v^{sqr}_m - v^{sqr}_n = 2(R_{mn}\cdot P_{mn} + X_{mn}\cdot Q_{mn}) + Z^2_{mn}\cdot i^{sqr}_{mn} \qquad \forall mn\in L,\forall m\in N,\forall n\in N \qquad (23)$$

$$v^{sqr}_n\cdot i^{sqr}_{mn} = P^2_{mn} + Q^2_{mn} \qquad \forall mn\in L,\forall n\in N \qquad (24)$$

$$V^2_{\min}\le v^{sqr}_n\le V^2_{\max} \qquad \forall n\in N \qquad (25)$$

$$0\le i^{sqr}_{mn}\le I^2_{\max} \qquad \forall mn\in L \qquad (26)$$

$$0\le P^G_n\le P^G_{\max} \qquad \forall n\in N \qquad (27)$$

$$PE_n = PEVCS.y_h \qquad \forall n\in N\quad \forall h\in J\quad \forall n\in N,\forall j\cap N \qquad (28)$$

$$P^h_{ficticia}\ge 0 \qquad \forall h\in V \qquad (29)$$

The objective function in Eq. (1) seeks to minimize the summation of four terms. The first term is the construction and maintenance cost of an EVCS at node *h*. The second term is the routing cost performed by the vehicle *k* from node *g* to node *h*. In this term the maintenance in terms of the distance traveled by the EV is also considered. The third term is a penalization created in case of need to increase the battery autonomy in EVs, in order to complete the routing and deliver the merchandise to customers. This term is the cost to make the problem feasible and is defined as the product between a positive variable $P^{ficticious}_{hk}$ (Increase of the battery autonomy at vehicle *k* to arrive node *h*) and the cost ap_k of the additional capacity of the battery. The last term represents the cost of the energy losses increase through the PDS lines compared with the energy losses when no EVCSs were installed (Benchmark case). Note that the four terms of the objective function are defined in Eqs. (2-5) respectively, along a period equal to one year and shifted to future value. This latter depends on the number of years *nt* the cost will be shifted to future and the Consumer Price Index *CPI*. Weighting factors W_1, W_2, W_3 and W_4 in objective function provide a level of importance for each term, making the summation of all of them equals to the unity. The values assigned to these factors depend on strategic data managed by decision maker in the integrated planning. This information is related with financial availability to implement the routing, EVCSs construction, battery technology, between others. The values that best represent the deal between objectives can be obtained via a multi-objective approach, in order to build up an optimal front of solutions (which is not into the scope of this work). In the proposed model, punctual values for these factors are used in all instances and runs, distributing the relative importance of each factor in objective function, in such a way that the need to increase the battery autonomy is largely penalized and the routing cost is of greater importance than EVCSs installation and energy losses costs. Thus, in this proposal it is assumed that $W_3 > W_2 > W_1 = W_4$. Factor W_3 has the highest relevance, as it is attempted that a change of the battery capacity is not attractive. W_2 is greater than W_1 as the solution space of the routing is less restricted than the solution space of the EVCSs installation. Therefore, the aim is to prioritize routing over the EVCSs installation.

The constraint in (6) requires every arc to be traveled only once, while constraint in Eq. (7) is an inequality to warranty that EVs only recharge their batteries at a located EVCS. Eq. (8) is a constraint that assures the flow for each vehicle at each node. In (9), it is shown that the quantity of vehicles leaving the depot has to be the same as the number of vehicles entering the depot. Constraint in Eq. (10) requires each vehicle to do one trip at most. In (11), the cardinality of set *K*, assures that the maximum quantity of vehicles leaving the depot is limited by the quantity of vehicles available.

When vehicles visit an EVCS without merchandise demand, q_h=0, $h \epsilon J$. Constraint in Eq. (12) represents that the summation of the remaining load u_{ghk} of an EV entering an EVCS is equal to the remaining load of the vehicle leaving an EVCS. This guarantees the vehicle capacity balance and indicates that an EVCS can be revisited more than once. The change in the remaining load of an EV when entering a customer node (with $q_h \geq 0$) is calculated by constraint (13). If the vehicle *k* visits customer *h*, the remaining cargo is reduced by customer demand q_h. If the customer *h* is not visited by vehicle *k*, the constraint keeps valid. Both, constraints in (12) and (13) make an EV to pass by an EVCS more than once but visit a customer only once, and eliminate the generation of subtours. Constraint in (14) contains the range for u_{ghk} that can be at most, the total cargo capacity of the EV. Since the point of view of the EV battery, constraint in (15) records the EV battery autonomy in terms of distance. When the vehicle *k* with a battery autonomy *Q*, travels along the arc *gh*, the battery autonomy before entering node *h* pb_{hk}^1, is the subtraction between the battery range after leaving node *g* pb_{gk}^2 and the distance traveled d_{gh} along the arc.

Constraint (16) indicates that all the vehicles have to leave the depot with batteries completely charged. This also applies for the EVCSs, where constraint (17) describes that a vehicle will have its battery fully charged once leaving from the EVCS. Right before an EV enters a customer node, the battery autonomy will be the same once it leaves the node, which is established in constraint (18). If the vehicle does not have enough autonomy to arrive to the next node, a variable called $P_{hk}^{ficticious}$ is in charge to provide the missing autonomy. This latter is introduced in the objective function as a penalization, motivating the installation of EVCSs instead of to increase the EVs battery autonomy. In Eq. (19) the non-negativity of the battery autonomy is declared, and the binary decision variables are shown in Eq. (20). From Eq. (21) to Eq. (27) the status of the PDS is assessed. The balance of active and reactive power is done in Eq. (21) and Eq. (22) respectively. The voltage drop along the network segment *mn* is computed in (23) and the current square is obtained with constraint (24). The constraints from (25) to (28) determine the voltage limits for each node, current flowing through the lines, active power generated and power consumed by the EVCSs, being *PEVCS* the maximum power consumed by each EVCS. The non-negativity of the battery autonomy added to EV is formulated in Eq. (29).

3. Test systems and EVS-IPP mathematical model validation

In order to validate the mathematical model proposed, three different instances composed by combination of transportation networks and power distribution systems from the specialized literature are proposed. The characteristics of the transportation, power distribution and hybrid networks, are featured below. Some tests are carried out on the uncoupled instances.

3.1. Transportation networks test systems

In this study, small-size instances for CVRP are used to examine the EVs-IPP mathematical model since the transportation network approach. As shown in (Yang and Sun 2015), three instances are generated from the *Pn16k8* instance, available in (NEO Networking and Emerging Optimization 2013). Instead of using all customers in the instance, each instance contains only a certain number of customers. For example, in this work, *Pn6k2* presents the last 6 customers of *Pn16k8*, *Pn7k3* presents the last 7 customers of *Pn16k8* with 3 vehicles, and *Pn8k3* contains the last 8 customers of *Pn16k8* with 3 vehicles (Table 1). According to the tests performed in (Yang and Sun 2015), the autonomy Q for the EV's battery is set in $[1.2d_{max}]$, being d_{max} the maximum Euclidean distance between any two nodes in the network. The cost associated with an EVCS construction is $[0.5Q]$. In this case, it is assumed that all the customer nodes are candidates for EVCSs.

Table 1
Small-size transportation network instances

Instance						Coord.X	Coord.Y
Pn6k2		Pn7k3		Pn8k3			
Customer node	EVCS candidate node	Customer node	EVCS candidate node	Customer node	EVCS candidate node		
				1	9	57	58
		1	8	2	10	62	42
1	7	2	9	3	11	42	57
2	8	3	10	4	12	27	68
3	9	4	11	5	13	43	67
4	10	5	12	6	14	58	48
5	11	6	13	7	15	58	27
6	12	7	14	8	16	37	69
Depot (0 and 0')						1	-1

Table 2 provides the results obtained by EVs-IPP in *Pn6k2*, *Pn7k3* and *Pn8k3* instances, which can also be found in (Yang and Sun 2015). Note that the candidate nodes where EVCSs were installed at are underlined along the EVs routes described in the column "Route".

Table 2
Results for three different transportation network instances

Instance	EVCSs installed	Objective function	Route			Time [s]
			k=1	k=2	k=3	
Pn6k2	2	426.8609	0-<u>10</u>-4-5-0'	0-1-<u>9</u>-3-6-2-0'		21
Pn7k3	2	428.5961	0-6-1-<u>12</u>-5-0'	0-3-7-<u>14</u>-4-2-0'		688
Pn8k3	2	597.1575	0-4-<u>16</u>-8-5-3-0'	0-7-2-<u>14</u>-0'	0-1-6-<u>14</u>-0'	352

3.2. Power distribution test systems

By the side of power distribution networks, three test systems from the literature were used. The first system can be found in (Civanlar et al., 1988). This instance is a three-feeder system with 16 nodes, which will be named DS16N. The second test system is a 34-nodes feeder (named in this work DS34N) available in (RIBEIRO 2013), rated at 11kV and utilized by other authors in optimal location of capacitors. The third case (named DS23N in this work), with 23 nodes, is a two-feeder distribution system (Miranda et al., 1994) rated at 28kV.

Considering the effect of the power distribution system in EVs-IPP mathematical model, the electric feeders mentioned above are coupled with a transportation network. No matter which transportation network is used for this test, if a big autonomy Q for the EVs' batteries is used, the vehicles are able to complete the routes and meet the customers, without the need to install any EVCSs. In this sense, the results (voltage profile) since the point of view of the power distribution system will be quite similar as those that can be obtained with the conventional back-forward sweep algorithm, as there are no additional power loads. The error in p.u. between the voltage calculated by back-forward sweep algorithm and the EVs-IPP mathematical model is shown in Figs. 1-3 for DS16N, DS34N, DS23N test systems respectively.

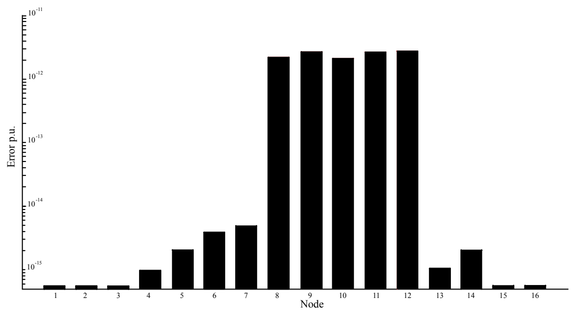

Fig. 1. Voltages error in p.u. for DS16N test system between backward-forward sweep algorithm and EVs-IPP mathematical model

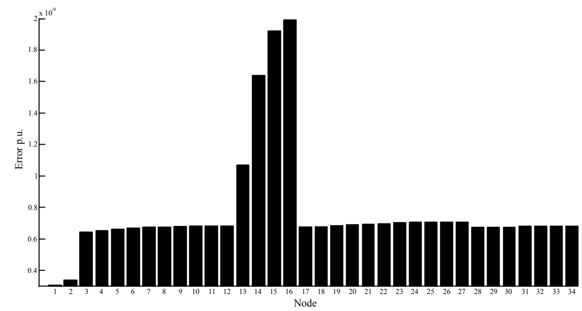

Fig. 2. Voltages error in p.u. for DS34N test system between backward-forward sweep algorithm and EVs-IPP mathematical model

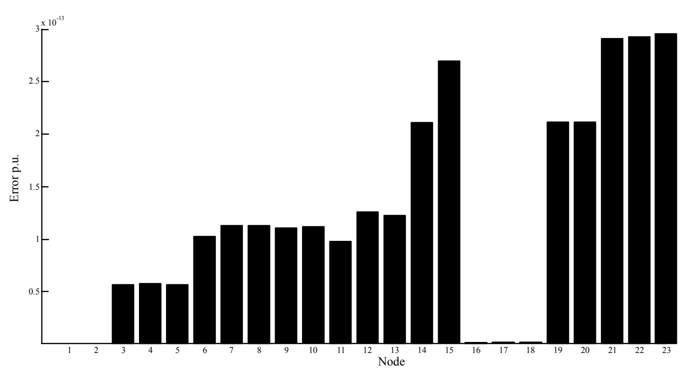

Fig. 3. Voltages error in p.u. for DS23N test system between backward-forward sweep algorithm and EVs-IPP mathematical model

Since the lower limit of voltage constraint in EVs-IPP mathematical model is not reached, the voltage at nodes are very similar compared with the voltage obtained with backward-forward sweep algorithm, as this latter is not able to restrict this variable. Figs. (1-3) depict that the maximum error between the two methods is 1.9928×10^{-9}.

3.3. Coupled systems

In order to examine the EVs-IPP's capability from a general perspective, both electric and transportation networks are coupled. Therefore, three new instances are created from the power networks and transportation instances shown before. These new instances are exposed in detail in (Power Systems Planning Group n.d.). Fig. 4 shows the coupling between *Pn6k2* and *DS16N*. Note that nodes joined with continuous line represent the power distribution system, being nodes 7, 8 and 9 the distribution substations. The transportation network is portrayed by the square nodes. Fig. 5 presents the coupling between *Pn7k3* and *DS34N*, where node 8 is the distribution substation. Finally, coupling of *Pn8k3* and *DS23N* is shown in Fig. 6, with two distribution feeders around the transportation network compound by 8 nodes. In all three instances, it is assumed that none of the PDS nodes is located at the same coordinates of the customers. Therefore, EVCSs are not able to be installed on the customers' nodes (as EVCSs draw power from electric grid), which implies that the EV is required to visit a power network node (to an installed EVCS) once the battery is almost depleted and returns to still visiting the customers.

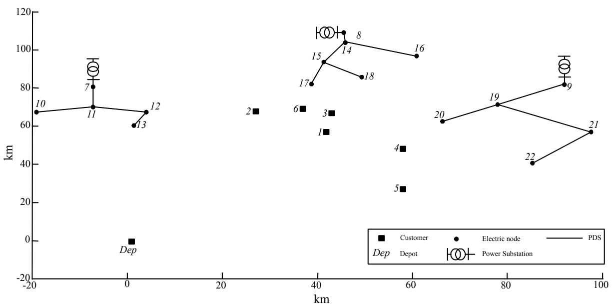

Fig. 4. Coupling between *Pn6k2* and *DS16N*

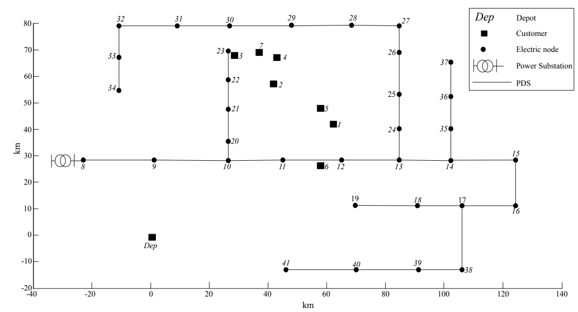

Fig. 5. Coupling between *Pn7k3* and *DS34N*

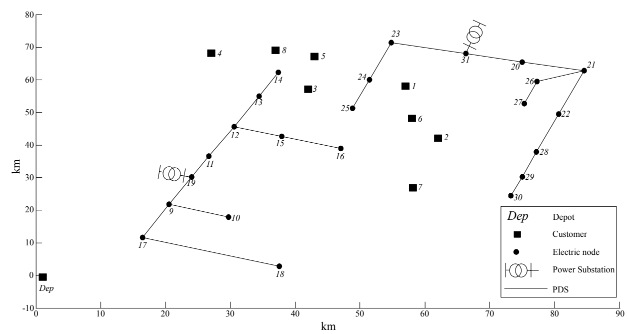

Fig. 6. Coupling between *Pn8k3* and *DS23N*

4. Results

Coupled systems shown in Figs. (4-6), are utilized to assess the performance of EVs-IPP. Parameters for all three instances were chosen consistently to the reality. According to (Tesla Supercharger 2017), an EVCS may draw from the PDS up to 120 kW for a 272 km battery-range. In this work, *PEVCS* used is 60 kW, as the average range evaluated in the runs is around 130 km, considering a linear behavior between maximum power at EVCS and distance that can be traveled. The cost f_h related with EVCS construction is assumed to be 22000 USD, as established in (Agenbroad 2014), taking into account type of installation, materials, connectivity, data and other factors. Parameter fm_h, which is the maintenance cost associated with this infrastructure, is around 10% the installation cost. Since the point of view of the EV operation, the average cost is 2.423 USD to travel 100 km, as reported by (U.S. Department of Energy 2017), and an estimation of 86 USD for EV maintenance every 5000 km traveled. The parameter ap_k is chosen arbitrarily as 1000 times the cost per kilometer travelled, in order to strongly penalize the third term in the objective function. By the hand of PDS losses, the power losses cost used in all cases is 4.34 Cents per kWh. To shift the cost to future value, *CPI* is set in 5%. Weighting factors assigned in the objective function at all runs are: W_1=0.1, W_2=0.2, W_3=0.6 and W_4=0.1. There is a high weight for the third term in objective function, in comparison to the other terms, as the purpose is to obtain a solution where the EVCSs installation be encouraged instead of change the EVs' battery for a battery with larger autonomy. The proposed EVs-IPP model has been programmed and executed in the GAMS (*General Algebraic Modeling System)* environment (GAMS Development Corporation 2016) on a HP desktop computer, Windows 64-bit operating system, with an Intel Core i3 @ 3.3 GHz processor and 4 GB of RAM. The presence of nonlinearities and integer and continuous variables into equations, make the proposed EVs-IPP model be a MINLP, which is solved using the DICOPT solver (GAMS Development Corporation 2016).

4.1. *Pn6k2-DS16N*

The results for instance *Pn6k2-DS16N* are presented in Table 3, considering different values of battery autonomy Q and three values for parameter M described in equation (7). This parameter restricts the number of arcs entering and leaving an EVCS, limiting indirectly the number of vehicles that can visit the EVCS. For example, if $M=1$, one EV is allowed to visit the EVCS. If $M=2$, only two EVs are permitted to enter an EVCS, and if $M=150$ (or a big number), all the EVs in the routing problem can visit the EVCS.

Table 3
Results for instance *Pn6k2-DS16N*

Q [km]	α [USD]	β [USD]	ω [USD]	Details of route		M	Time [s]
				k=1	k=2		
65	154430	483983	3515056	0-5-**22**-**19**-1-**20**-4-0'	0-**13**-2-3-**17**-6-0'	1	809
80	247088	663491	4454116	0-**11**-**14**-3-6-2-**12**-0'	0-**10**-1-**20**-4-5-**22**-**19**-**13**-0'	1	1940
90	185316	600830	2862231	0-**13**-3-6-2-**12**-0'	0-**11**-1-**20**-4-5-**19**-**10**-0'	1	860
100	92658	423713	1355481	0-**12**-1-3-6-2-**10**-0'	0-5-**20**-4-0'	1	177
110	92658	450983	1112783	0-1-**20**-5-0'	0-4-**19**-3-6-2-**10**-0'	1	112
120	61772	419941	728485	0-2-6-3-**20**-4-0'	0-1-**19**-5-0'	1	70
130	61772	420425	728485	0-2-6-3-**19**-0'	0-1-**20**-4-5-0'	1	67
140	61772	413734	717722	0-4-**19**-5-0'	0-**10**-2-6-3-1-0'	1	114
150	61772	413734	717722	0-1-3-6-2-**10**-0'	0-5-**19**-4-0'	1	164
160	30886	356486	381939	0-4-5-0'	0-1-3-6-2-**10**-0'	1	10
170	30886	356486	381939	0-1-3-6-2-**10**-0'	0-4-5-0'	1	18
180	0	324905	0	0-5-4-0'	0-2-6-3-1-0'	1	5
200	0	324905	0	0-2-6-3-1-0'	0-5-4-0'	1	5
65	123544	566686	3171244	0-**13**-2-3-**17**-6-0'	0-**13**-**17**-1-**20**-**22**-5-**22**-**20**-4-0'	2	709
80	92658	571488	1355481	0-**10**-**20**-4-5-**20**-1-**10**-0'	0-**12**-3-6-2-**12**-0'	2	136
90	92658	571055	1355481	0-**10**-6-3-2-**12**-0'	0-**12**-1-**20**-5-4-**20**-**10**-0'	2	403
100	61772	426025	773007	0-4-**20**-5-0'	0-1-**20**-3-6-2-**10**-0'	2	41
110	61772	426025	773007	0-1-**20**-5-0'	0-**10**-2-6-3-**20**-4-0'	2	149
120	30886	394444	388708	0-4-**20**-5-0'	0-1-**20**-3-6-2-0'	2	31
130	30886	394444	388708	0-1-**20**-5-0'	0-4-**20**-3-6-2-0'	2	40
140	30886	394444	388708	0-1-**20**-3-6-2-0'	0-4-**20**-5-0'	2	47
150	30886	394444	388708	0-4-**20**-3-6-2-0'	0-1-**20**-5-0'	2	23
160	30886	356486	381939	0-5-4-0'	0-**10**-2-6-3-1-0'	2	19
170	30886	356486	381939	0-4-5-0'	0-1-3-6-2-**10**-0'	2	18
180	0	324905	0	0-1-3-6-2-0'	0-4-5-0'	2	5
200	0	324905	0	0-5-4-0'	0-1-3-6-2-0'	2	5
65	123544	649628	2133795	0-**13**-**12**-**20**-**22**-5-**22**-4-**20**-**12**-**13**-0'	0-**13**-**12**-1-**20**-3-6-2-**12**-**13**-0'	150	109
80	61772	542047	968403	0-**12**-**20**-4-5-**20**-1-**12**-0'	0-**12**-3-6-2-**12**-0'	150	54
90	61772	542047	968403	0-**12**-2-6-3-**12**-0'	0-12-1-**20**-4-5-**20**-0'	150	112
100	30886	449419	388708	0-**20**-3-6-2-1-**20**-0'	0-5-**20**-4-0'	150	28
110	30886	449419	388708	0-**20**-3-6-2-1-**20**-0'	0-4-**20**-5-0'	150	29
120	30886	394444	388708	0-2-6-3-**20**-1-0'	0-4-**20**-5-0'	150	21
130	30886	394444	388708	0-2-6-3-**20**-4-0'	0-5-**20**-1-0'	150	24
140	30886	394444	388708	0-4-**20**-5-0'	0-1-**20**-3-6-2-0'	150	33
150	30886	394444	388708	0-2-6-3-**20**-4-0'	0-1-**20**-5-0'	150	27
160	30886	356486	381939	0-4-5-0'	0-1-3-6-2-**10**-0'	150	13
170	30886	356486	381939	0-**10**-2-6-3-1-0'	0-4-5-0'	150	20
180	0	324905	0	0-1-3-6-2-0'	0-5-4-0'	150	3
200	0	324905	0	0-1-3-6-2-0'	0-4-5-0'	150	3

According to Table 3, as the battery autonomy (first column) is increased for a certain value of M (column 7), there is a reduction of the cost associated with EVCS installation, EVs routing and PDS energy losses (second, third and fourth columns respectively). Columns 5 and 6 show the nodes sequence traveled by the EVs, with the EVCSs identified in **bold**. When the battery autonomy Q is large enough (Q>180 km), no EVCSs are installed and the terms α and ω are zero, obtaining the same results as those presented in benchmark case. Fig. 7 depicts the EVs routes and the EVCSs installed along the PDS for instance *Pn6k2-DS16N*, with Q=80 km and $M=1$. Note that the EVCSs are allowed to be visited by one EV. After visiting EVCS in 11, EV1 has to visit another EVCS located at node 14, as the recharge acquired in 11 is not sufficient to visit all customers and come back to the depot. For values of Q greater or equal than 80 km, the third term γ of the objective function is always zero. For values of Q less than 80 km, i.e., Q=65 km in Table 3, the term γ is greater than zero. This situation suggests an upgrade in the battery, because along the routes, the autonomy for both EVs is not sufficient to complete some arcs and installing more EVCSs could incur in a relevant increase of energy losses (installation of EVCSs at nodes quite far from the substation). Specifically, for Q=65 km and M=150, the route traveled by EV1 is the longest path found in all the runs shown in Table 3. Due to M has a big number, there are more options to go back to depot after visiting customers and the routing length becomes longer than other cases. In contrast with this case, the routing length is smaller for Q=65 km and M=1, as the EVCS revisit is not permitted, reducing the options for EVs to go back to depot.

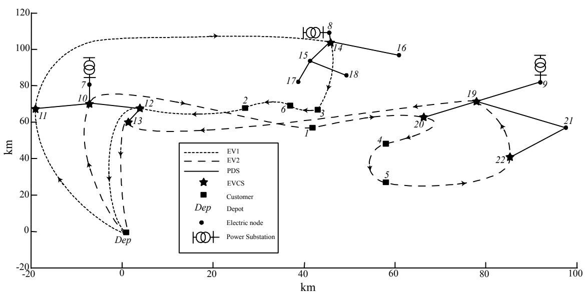

Fig. 7. *Pn6k2-DS16N* with M=1 and Q=80 km

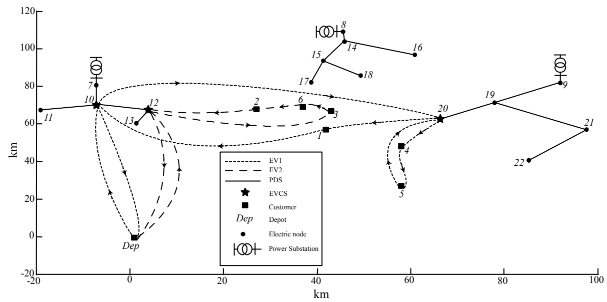

Fig. 8. *Pn6k2-DS16N* with M=2 and Q=80 km

For M=2 and Q=80 km, the graphic result is shown in Fig. 8. Due to M=2, the number of arcs entering and leaving an EVCS installed can be less or equal than 2. Even if M=2 some of the EVCSs receive one vehicle, which visits the EVCS, then goes to visit other customers and come back to the same EVCS to recharge the battery and continue with the travel. This case applies for EV2, which once leaves from node 12 (EVCS installed), visits the customers at nodes 3, 6 and 2, and returns to node 12. The same situation happens for EV1, when revisits EVCS installed at node 20 after visiting customers at nodes 4 and 5. When M=150 and Q=80 km, the behavior is pretty the same as that presented in Fig. 8. While for M=2, EV1 visits the EVCS installed at node 10, the routing sequence (see this case in Table 3) changes slightly when M=150, as EV1 visits EVCS at node 12 (which is also visited by EV2). This is the result of relaxing the parameter M with a big number, allowing the EVCS to receive several EVs. In this sense, the number of EVCSs is reduced, resulting in the decrease of energy losses in PDS.

4.2. Pn7k3-DS34N

Following the same dynamic with *Pn6k2-DS16N,* the results for *Pn7k3-DS34N* are presented in Table 4. In this latter, the execution time increases compared with *Pn6k2-DS16N* for the majority of the cases, because the introduction of more customers and vehicles (since the transportation approach), and the enlargement of the PDS contributes to a greater degree of the computational effort. In some cases all the three vehicles are used. For those runs where Q<120 km, Q<90 km and Q<30 km for M=1, M=2 and M=150 respectively, the solver failed and was not able to find a feasible solution after too long. Considering the situation in which M=150 and Q=30, the graphic solution is depicted in Fig. 9. It is noted from this case that the EVCSs are installed as closest as possible to the power substation located at node 8, as a measure to reduce energy losses. By the other side, the revisit is done in all the ECVSs installed, due to relaxation of constraint in Eq. (7) by increasing parameter M.

Table 4
Results for instance *Pn7k3-DS34N*

Q [km]	α [USD]	β [USD]	ω [USD]	Details of route k=1	k=2	k=3	M	Time [s]
120	61772	338027	2194760	0-6-1-5-**21**-0'	0-2-4-7-3-**22**-0'		1	11882
130	61772	327429	2073954	0-6-1-5-**10**-0'	0-3-7-4-2-**20**-0'		1	5691
140	61772	432216	1556729	0-3-7-**9**-2-4-0'	0-6-1-5-**10**-0'		1	5839
150	61772	330324	1556729	0-2-4-7-3-**9**-0'	0-**10**-5-1-6-0'		1	5730
160	30886	449912	537845	0-6-0'	0-2-4-7-3-**9**-0'	0-5-1-0'	1	626
170	0	466447	0	0-6-1-5-0'	0-3-0'	0-7-4-2-0'	1	27
180	0	326609	0	0-3-7-4-2-0'	0-6-1-5-0'		1	39
200	0	352291	0	0-7-3-2-4-0'	0-6-1-5-0'		1	11
90	61772	346245	2106560	0-**10**-6-1-5-**21**-0'	0-**21**-3-7-4-2-**10**-0'		2	32122
100	61772	337444	2073954	0-**10**-6-1-5-**10**-0'	0-**20**-2-4-7-3-**20**-0'		2	22598
110	61772	397053	1556729	0-**9**-3-7-4-2-**10**-0'	0-**9**-5-1-**10**-6-0'		2	27553
120	30886	339063	1084099	0-0'	0-6-1-5-**21**-0'	0-**21**-3-7-4-2-0'	2	1329
130	30886	329757	1051509	0-3-7-4-2-**20**-0'	0-6-1-5-**20**-0'		2	818
140	30886	327851	1017078	0-6-1-5-**10**-0'	0-3-7-4-2-**10**-0'		2	1002
150	30886	343577	537845	0-6-1-5-**9**-0'	0-2-4-7-3-**9**-0'		2	299
160	30886	343577	537845	0-**9**-3-7-4-2-0'	0-6-1-5-**9**-0'		2	103
170	0	466447	0	0-7-4-2-0'	0-5-1-6-0'	0-3-0'	2	82
180	0	326609	0	0-2-4-7-3-0'	0-5-1-6-0'		2	27
200	0	326609	0	0-0'	0-6-1-5-0'	0-3-7-4-2-0'	2	29
30	185316	509999	7986105	0-**9**-**20**-**11**-6-**12**-1-**12**-5-**12**-**11**-**20**-**9**-	0-**9**-**20**-**22**-2-**22**-3-**23**-4-**23**-7-**22**-**20**-**9**-		150	28010
60	61772	367532	2820349	0-**11**-5-1-6-**11**-0'	0-**21**-7-4-2-**21**-3-**21**-0'		150	6728
80	30886	426192	1084099	0-**21**-1-5-**21**-6-**21**-0'	0-**21**-2-4-7-3-**21**-0'		150	2683
90	30886	346314	1051509	0-**20**-2-4-7-3-**20**-0'	0-**20**-5-1-6-**20**-0'		150	411
100	30886	339333	1017078	0-**10**-6-1-5-**10**-0'	0-**10**-3-7-4-2-**10**-0'		150	1825
110	30886	339333	1017078	0-**10**-5-1-6-**10**-0'	0-**10**-2-4-7-3-**10**-0'		150	197
120	30886	339333	1017078	0-**10**-6-1-5-**10**-0'	0-**10**-2-4-7-3-**10**-0'		150	562
130	30886	453507	537845	0-**9**-2-4-7-3-**9**-0'	0-**9**-1-5-**9**-6-0'		150	177
140	30886	373938	537845	0-**9**-3-7-4-2-**9**-0'	0-**9**-6-1-5-**9**-0'		150	194
150	30886	343577	537845	0-6-1-5-**9**-0'	0-**9**-3-7-4-2-0'		150	88
160	30886	343577	537845	0-6-1-5-**9**-0'	0-2-4-7-3-**9**-0'		150	61
*160	30886	505182	3438866	0-3-7-4-**35**-1-0'	0-6-**35**-5-2-0'		150	9112
170	0	466447	0	0-6-1-5-0'	0-7-4-2-0'	0-3-0'	150	53
180	0	326609	0	0-5-1-6-0'	0-2-4-7-3-0'		150	35
200	0	326609	0	0-5-1-6-0'	0-2-4-7-3-0'		150	16

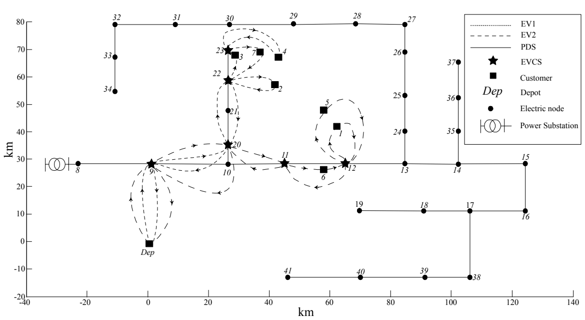

Fig. 9. *Pn7k3-DS34N* with M=150 and Q=30 km

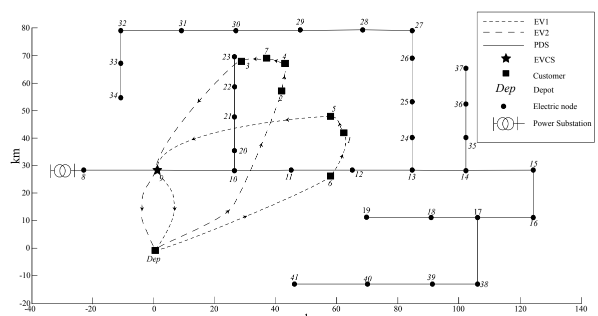

Fig. 10. *Pn7k3-DS34N* with M=150 and Q=160 km

Note from Table 4 that this run has the longest computational time (around 8 hours) to obtain a solution, because the autonomy is slightly bigger than the distance between the depot and the closest electric node where an EVCS should be installed (*dist(Dep-9)*=29.33 km). This fact contributes that finding a feasible solution be hard as the battery autonomy is barely enough to complete the route. Looking into a larger autonomy, Fig. 10 represents the solution with M=150 and Q=160. In this situation, the behavior is consistent in regards the location of the EVCS close to the power substation (at node 9). See that only one EVCS is installed to virtually increase the battery autonomy and meet the customers. However, other situations should be studied, for example: Fig. 11 shows that a large portion of the nodes (area shaded) belonging PDS are not allowed to install EVCSs (nodes from 9 to15 and from 20 to 30) due to other issues (limitations associated with terrain topology, public space, right of way, etc.) that are not addressed in this work. In this sense, the EVCS should be installed at the node where the energy losses be as reduced as possible. The solution shows that this can be reached by installing the EVCS at node 35, which is the next node out of the restricted area and with a less distance to the substation, compared with nodes 31, 32, 33 and 34. The costs and sequence of routes obtained for this solution are found in Table 4 at Q=*160 km.

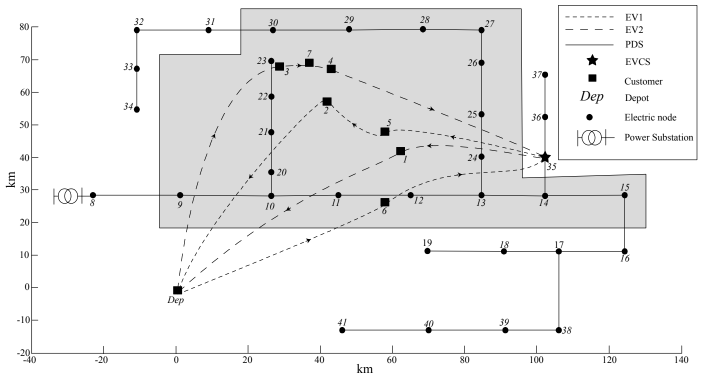

Fig. 11. *Pn7k3-DS34N* with M=150 and Q=160 km, restricting EVCSs at nodes 9-15 and 20-30

4.3. Pn8k3-DS23N

As mentioned before, the addition of a new customer to the transportation network, contributes to increase computational effort for finding a solution, which can be seen in Table 5 for instance *Pn8k3-DS23N*.

Table 5
Results for instance *Pn8k3-DS23N*

Q [km]	α [USD]	β [USD]	ω [USD]	Details of route			M	Time [s]
				k=1	k=2	k=3		
160	30886	492614	305791	0-**11**-1-6-0’	0-7-2-0’	0-**11**-3-8-5-4-0’	2	16280
170	0	489870	0	0-5-8-4-0’	0-6-2-7-0’	0-1-3-0’	2	218
180	0	482567	0	0-4-8-5-3-0’	0-1-6-0’	0-2-7-0’	2	245
60	61772	564356	996107	0-**11**-1-**25**-**11**-0’	0-**11**-7-**25**-3-4-**11**-0’	0-**11**-2-6-25-5-8-**11**-0’	150	19686
70	61772	605522	636591	0-**11**-3-**23**-1-**11**-0’	0-**11**-7-**11**-4-**11**-0’	0-**11**-2-6-**23**-5-8-**11**-0’	150	6999
80	30886	616619	305791	0-**11**-7-**11**-2-6-**11**-0’	0-**11**-3-5-8-**11**-4-**11**-0’	0-**11**-1-**11**-0’	150	7487
90	30886	510102	305791	0-**11**-1-**11**-0’	0-**11**-6-2-7-**11**-0’	0-**11**-4-8-5-3-**11**-0’	150	1133
100	30886	510102	305791	0-**11**-6-2-7-**11**-0’	0-**11**-1-**11**-0’	0-**11**-3-5-8-4-**11**-0’	150	718
110	30886	510102	305791	0-**11**-7-2-6-**11**-0’	0-**11**-1-**11**-0’	0-**11**-3-5-8-4-**11**-0’	150	1337
120	30886	494395	305791	0-7-2-6-**11**-0’	0-**11**-3-5-8-4-**11**-0’	0-1-**11**-0’	150	791
130	30886	490312	305791	0-6-1-**11**-0’	0-**11**-2-7-0’	0-4-8-5-3-**11**-0’	150	10297
140	30886	490312	305791	0-6-1-**11**-0’	0-4-8-5-3-**11**-0’	0-7-2-**11**-0’	150	189
150	30886	490312	305791	0-**11**-1-6-0’	0-**11**-3-5-8-4-0’	0-7-2-**11**-0’	150	3866
160	30886	483843	305791	0-2-7-0’	0-6-1-**11**-0’	0-4-8-5-3-**11**-0’	150	318
170	0	489870	0	0-6-2-7-0’	0-3-1-0’	0-4-8-5-0’	150	64

Even if the mathematical model is relaxed with M=150 for constraint in (7), run time is notably long compared with the instances *Pn6k2-DS16N* and *Pn7k3-DS34N* for similar cases of battery autonomy Q. It is not possible for solver to find a solution for cases when M=1 (not presented in Table 5) and the installation of EVCSs is required, i.e., when the solution is different from the benchmark case. By the other side, when M=2 and Q<160 km no solution is found, because the number of customers and limitation in parameter M (which greatly restricts the mathematical model) makes impossible to get at least a feasible solution, due to an exact solution technique is being used. Routing solution with M=2 and Q=160 km is shown in Fig. 12. See that Q is barely sufficient to complete a big portion of the routes length, being necessary the installation of only one EVCS for EV2 and EV3. EV1 is able to meet its respective customers with autonomy assigned.

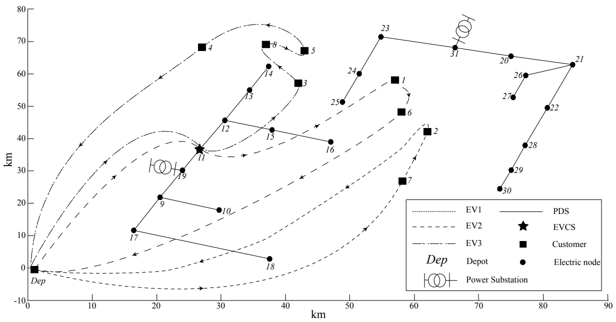

Fig. 12. *Pn8k3-DS23N* with *M*=2 and *Q*=160 km

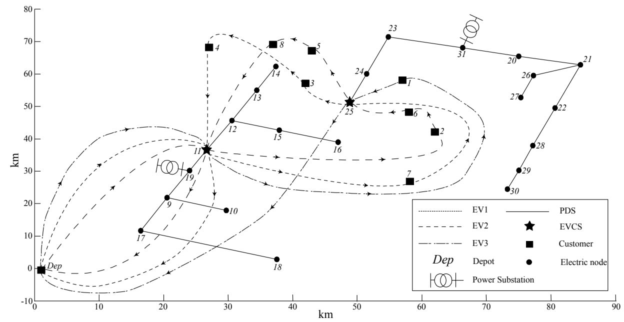

Fig. 13. *Pn8k3-DS23N* with *M*=150 and *Q*=60 km

In contrast with case mentioned above, Fig. 13 illustrates a different situation in which *M* is increased (relaxed mathematical model) and autonomy is reduced. For *M*=150 and *Q*=60 km, the installation of two EVCSs is required at both feeders of the PDS. According to Table 5, it is worth to mention that in this case the cost for energy losses is increased in three times compared with situation shown in Fig. 12. Likewise, it is noted that both EVCSs are visited by all EVs to renew autonomy and meet customers.

5. Conclusions

This paper presented an electric vehicle integrated planning problem (EVs-IPP) model to improve the performance of transportation network and power distribution system PDS. A sensitivity analysis was performed by relaxing mathematical model and using different values of EVs' battery autonomy. In this manner, the number of EVs permitted to be recharged at a given EVCS was under control, examining different costs for each solution, i.e., EVCSs installed along the PDS, EVs routing and energy losses. The cases in which was not necessary to install EVCSs due to the high battery autonomy, the results related with routing (transportation network approach) and power flow (PDS approach) were quite similar to those obtained in the benchmark case. By restricting some nodes at the PDS, EVCSs were located as closest as possible to the power feeder substation, in order to make minimum the energy losses. The latter greatly contribute to objective function when the EVCSs are subjected to receive only one vehicle. In the cases, where a comparison with autonomy could be done, i.e., for *Pn6k2-DS16N* instance with *M=1*, the energy losses cost was 16 times greater than those presented when the EVCSs are able to receive all the EVs (*M*=150). Due to the existence of several terms in objective function, the problem could be treated since the point of view of the multi-objective optimization. By varying weighting factors, a set of solutions can be built up, represented along a Pareto front. However, the proposed model can be solved by using meta-heuristic techniques such as NSGA II, SPEA, Epsilon Constraint, among others, to find a front of solutions with different weights for each objective. In this work, concrete values for weighting factors in the objective function were used, in order to represent consistently the priorities established by the decision maker, which would be the owner of both, the transportation and power distribution networks. Otherwise, the problem should be dealt as a bi-level problem, where the solution of the routing and EVCSs installation costs would be the input to find the energy losses on the power flow formulation.

References

Agenbroad, J. (2014). Pulling Back the Veil on EV Charging Station Costs - Rocky Mountain Institute. *Rocky Mountain Institute*. https://www.rmi.org/news/pulling-back-veil-ev-charging-station-costs/ (June 1, 2017).

Arias, A., Martínez, L. H., Hincapie, R. A., & Granada, M. (2015, October). An IEEE Xplore database literature review regarding the interaction between electric vehicles and power grids. In *Innovative Smart Grid Technologies Latin America (ISGT LATAM), 2015 IEEE PES* (pp. 673-678). IEEE.

Chan, C. C. (1999). The past, present and future of electric vehicle development. In *Power Electronics and Drive Systems, 1999. PEDS'99. Proceedings of the IEEE 1999 International Conference on* (Vol. 1, pp. 11-13). IEEE.

Christofides, N., Mingozzi, A., & Toth, P. (1977). The vehicle routing problem. In *Combinatorial Optimization*,

Society for Industrial and Applied Mathematics, 315–38.
Civanlar, S., Grainger, J. J., Yin, H., & Lee, S. S. H. (1988). Distribution feeder reconfiguration for loss reduction. *IEEE Transactions on Power Delivery*, *3*(3), 1217-1223.
Dong, X., Mu, Y., Jia, H., Wu, J., & Yu, X. (2016). Planning of fast EV charging stations on a round freeway. *IEEE Transactions on Sustainable Energy*, *7*(4), 1452-1461.
Du, Y., Zhou, X., Bai, S., Lukic, S., & Huang, A. (2010, February). Review of non-isolated bi-directional DC-DC converters for plug-in hybrid electric vehicle charge station application at municipal parking decks. In *Applied Power Electronics Conference and Exposition (APEC), 2010 Twenty-Fifth Annual IEEE* (pp. 1145-1151). IEEE.
GAMS Development Corporation. (2016). GAMS Solvers. https://gams.com/latest/docs/solvers/index.html (June 1, 2017).
Hannan, M. A., Lipu, M. S. H., Hussain, A., & Mohamed, A. (2017). A review of lithium-ion battery state of charge estimation and management system in electric vehicle applications: Challenges and recommendations. *Renewable and Sustainable Energy Reviews*, *78*, 834-854.
Intergovernmental Panel on Climate Change. (2015). *Climate change 2014: mitigation of climate change* (Vol. 3). Cambridge University Press.
Liu, Z. F., Zhang, W., Ji, X., & Li, K. (2012, May). Optimal planning of charging station for electric vehicle based on particle swarm optimization. In *Innovative Smart Grid Technologies-Asia (ISGT Asia), 2012 IEEE* (pp. 1-5). IEEE.
Luo, C., Huang, Y. F., & Gupta, V. (2017). Placement of EV Charging Stations—Balancing Benefits Among Multiple Entities. *IEEE Transactions on Smart Grid*, *8*(2), 759-768.
Miranda, V., Ranito, J. V., & Proenca, L. M. (1994). Genetic algorithms in optimal multistage distribution network planning. *IEEE Transactions on Power Systems*, *9*(4), 1927-1933.
Mock, P. (2014). EU CO2 standards for passenger cars and light-commercial vehicles. *The International Council on Clear Transportation*.
NEO Networking and Emerging Optimization. (2013). VRP Instances: Vehicle Routing Problem. http://neo.lcc.uma.es/vrp/vrp-instances/ (June 1, 2017).
Neyestani, N., Damavandi, M. Y., Shafie-Khah, M., Contreras, J., & Catalão, J. P. (2015). Allocation of plug-in vehicles' parking lots in distribution systems considering network-constrained objectives. *IEEE Transactions on Power Systems*, *30*(5), 2643-2656.
Pazouki, S., Mohsenzadeh, A., Ardalan, S., & Haghifam, M. R. (2015). Simultaneous planning of PEV charging stations and DGs considering financial, technical, and environmental effects. *Canadian Journal of Electrical and Computer Engineering*, *38*(3), 238-245.
Power Systems Planning Group. (2017). Electric Vehicles Integrated Planning Problem Test Systems. http://academia.utp.edu.co/planeamiento/sistemas-de-prueba/evs-ipp/ (June 2, 2017).
Ribeiro, É. T. A. (2013). Modelos de programação inteira mista para a alocação ótima de bancos de capacitores em sistemas de distribuição de energia elétrica radias.
Shojaabadi, S., Abapour, S., Abapour, M., & Nahavandi, A. (2016). Optimal planning of plug-in hybrid electric vehicle charging station in distribution network considering demand response programs and uncertainties. *IET Generation, Transmission & Distribution*, *10*(13), 3330-3340.
Tanaka, N. (2011). Technology roadmap: Electric and plug-in hybrid electric vehicles. *International Energy Agency, Tech. Rep*.
Tesla Supercharger. (2017). https://www.tesla.com/supercharger (June 1, 2017).
U.S. Department of Energy. (2017). Alternative Fuels Data Center: Charging Plug-In Electric Vehicles at Home." *Energy Efficiency & Renewable Energy*. https://www.afdc.energy.gov/fuels/electricity_charging_home.html (June 1, 2017).
Worley, O., Klabjan, D., & Sweda, T. M. (2012, March). Simultaneous vehicle routing and charging station siting for commercial electric vehicles. In *Electric Vehicle Conference (IEVC), 2012 IEEE International* (pp. 1-3). IEEE.
Yang, J., & Sun, H. (2015). Battery swap station location-routing problem with capacitated electric vehicles. *Computers & Operations Research*, *55*, 217-232.